Aquifer Thermal Energy Storage (ATES) smart grids

Large-scale seasonal energy storage as a distributed energy management solution

Rostampour, Vahab; Jaxa-Rozen, Marc; Bloemendal, Martin; Kwakkel, Jan; Keviczky, Tamás

DOI
10.1016/j.apenergy.2019.03.110

Publication date
2019

Document Version
Final published version

Published in
Applied Energy

Citation (APA)
Rostampour, V., Jaxa-Rozen, M., Bloemendal, M., Kwakkel, J., & Keviczky, T. (2019). Aquifer Thermal Energy Storage (ATES) smart grids: Large-scale seasonal energy storage as a distributed energy management solution. *Applied Energy*, *242*, 624-639. https://doi.org/10.1016/j.apenergy.2019.03.110

Applied Energy 242 (2019) 624–639

Contents lists available at ScienceDirect

Applied Energy

journal homepage: www.elsevier.com/locate/apenergy

Aquifer Thermal Energy Storage (ATES) smart grids: Large-scale seasonal energy storage as a distributed energy management solution☆

Vahab Rostampour[a,*,1], Marc Jaxa-Rozen[b], Martin Bloemendal[c,d], Jan Kwakkel[b], Tamás Keviczky[a]

[a] Delft Center for Systems and Control, Delft University of Technology, Mekelweg 2, 2628 CD, Delft, the Netherlands
[b] Faculty of Technology, Policy and Management, Delft University of Technology, Jaffalaan 5, 2628 BX, Delft, the Netherlands
[c] Faculty of Civil Engineering and Geosciences, Delft University of Technology, Stevinweg 1, 2628 CN, Delft, the Netherlands
[d] KWR Watercycle Research Institute, Groningenhaven 7, 3433 PE, Nieuwegein, the Netherlands

HIGHLIGHTS

- Distributed control can dynamically manage thermal interferences between ATES wells.
- Information exchange enables denser ATES layouts without reducing efficiency.
- Specific GHG savings can be improved by 40% at the same level of thermal performance.

ARTICLE INFO

Keywords:
Aquifer Thermal Energy Storage (ATES)
Large-scale seasonal energy storage
Distributed energy management
Distributed probabilistic energy management
Distributed stochastic model predictive control

ABSTRACT

Aquifer Thermal Energy Storage (ATES) is a building technology used to seasonally store thermal energy in the subsurface, which can reduce the energy use of larger buildings by more than half. The spatial layout of ATES systems is a key aspect for the technology, as thermal interactions between neighboring systems can degrade system performance. In light of this issue, current planning policies for ATES aim to avoid thermal interactions; however, under such policies, some urban areas already lack space for the further development of ATES, limiting achievable energy savings. We show how information exchange between ATES systems can support the dynamic management of thermal interactions, so that a significantly denser layout can be applied to increase energy savings in a given area without affecting system performance. To illustrate this approach, we simulate a distributed control framework across a range of scenarios for spatial planning and ATES operation in the city center of Utrecht, in The Netherlands. The results indicate that the dynamic management of thermal interactions can improve specific greenhouse gas savings by up to 40% per unit of allocated subsurface volume, for an equivalent level of ATES economic performance. However, taking advantage of this approach will require revised spatial planning policies to allow a denser development of ATES in urban areas.

1. Introduction

Aquifer Thermal Energy Storage (ATES) is an innovative shallow geothermal energy technology, which can be used on a large scale to store thermal energy in natural subsurface formations. In combination with a heat pump, ATES can reduce energy use for heating and cooling by more than half in larger buildings [1], while supporting the electrification of building energy systems. This has made the technology increasingly popular in Northern Europe [2]. For instance, it is currently used in approximately 10% of new commercial and institutional buildings in The Netherlands, where ATES has been identified as a key technology towards long-term targets for greenhouse gas (GHG) emissions reductions in the built environment. Furthermore, the conditions required for ATES are relatively widespread across the globe; by the middle of the century, roughly half of the world's urban population is expected to live in areas with suitable subsurface and climate

☆ This research was supported by the Uncertainty Reduction in Smart Energy Systems (URSES) research program funded by the Dutch organization for scientific research (NWO) and Shell under the project Aquifer Thermal Energy Storage Smart Grids (ATES-SG) with grant number 408-13-030.

* Corresponding author.
E-mail address: v.rostampour@tudelft.nl (V. Rostampour).

[1] Vahab Rostampour and Marc Jaxa-Rozen contributed equally to this work.

https://doi.org/10.1016/j.apenergy.2019.03.110
Received 17 August 2018; Received in revised form 4 February 2019; Accepted 9 March 2019
Available online 19 March 2019

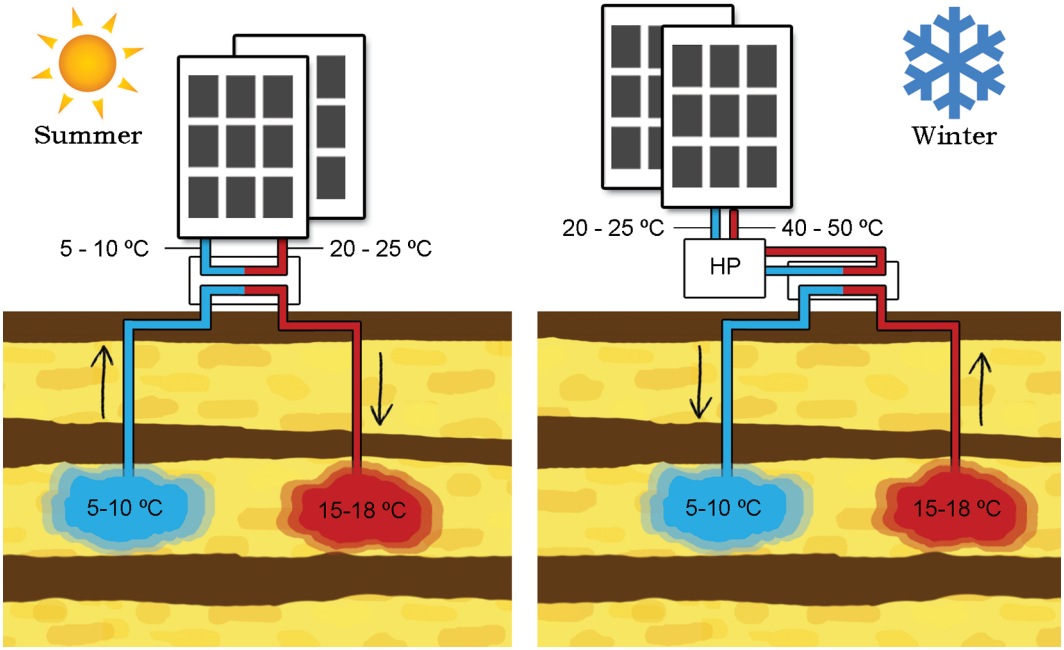

Fig. 1. Working principle of Aquifer Thermal Energy Storage.

conditions for ATES [3]. These areas include large parts of China and North America, where the large-scale deployment of ATES could significantly reduce total energy demand for space heating and cooling.

However, the progressive adoption of this technology in Europe has already evidenced some issues of concern for policymakers. The spatial layout and planning of the storage wells used in ATES is a key aspect for the management of the technology, as thermal interactions between neighboring systems which share an aquifer can affect their technical and economic performance. Current regimes for ATES management have therefore followed a highly conservative approach, to minimize the risk of a "tragedy of the commons" [4] – in which the overly dense development of ATES systems could lead to thermal interactions, and eventually degrade the potential of aquifers for thermal storage. However, recent research suggests that current planning methods are essentially incompatible with long-term objectives for the development of ATES in certain areas. For instance, several urban areas in The Netherlands already lack the space to accommodate further demand for ATES [5], although the technology's total market share is still only one-fifth of national policy objectives [6]. This situation presents a trade-off between public and private interests: while relaxed planning guidelines could contribute to GHG mitigation efforts by increasing the adoption of ATES, this could reduce the economic performance of the technology – and ultimately its long-term attractiveness as an energy-efficient option for building owners.

Improved methods for the management of ATES systems will therefore be needed to better align the interests of policymakers and building owners, and fulfill the technical potential of ATES. Current research on the larger-scale management of ATES has typically focused on the spatial layout and planning of storage wells; Sommer et al. for instance used an optimization approach to evaluate well layout configurations in idealized conditions [7], while Bloemendal et al. [5] assessed current planning practices in The Netherlands in light of simulation results for a wider range of well configurations. In parallel, Pophillat et al. [8] evaluated analytical methods which can support the integrated spatial planning of shallow geothermal energy by assessing the presence of thermal interactions. However, these studies used simplified representations of system operation and its links with spatial planning, and did not account for the potential of improved operating methods towards a more efficient resolution of the trade-off between public and private interests.

To this end, this paper introduces distributed ATES control as a starting point towards an improved regime for the management of ATES in urban areas, in which the exchange of information between neighbouring systems would support improved practices for the operation as well as the spatial planning of systems. This approach enables the dynamic management of thermal interactions in the subsurface – thus allowing a significantly denser spatial layout for ATES without affecting system performance, and increasing feasible energy savings from a given subsurface volume. To illustrate this approach, we develop and simulate a distributed energy management framework [9] under a range of scenarios for spatial planning and ATES operation, using a case study for the city of Utrecht, in The Netherlands.

The following section will frame the contributions of this paper in the context of key challenges for the development of ATES technology. This is followed by methods, a description of the case study, and simulation results. The last section of the paper builds on these results to outline policy recommendations, as well as directions for future work.

2. Background

2.1. Technical characteristics of ATES

Shallow geothermal systems are currently the fastest-growing application of geothermal energy [10]. These systems rely on the subsurface to extract or store thermal energy at depths of less than 500 m. Aquifer Thermal Energy Storage (ATES) is an increasingly popular form of shallow geothermal energy; ATES systems can be used to reduce building energy demand in temperate climates, by directly pumping groundwater for seasonal energy storage. As such, these systems typically involve at least one pair of coupled wells, which simultaneously infiltrate and extract groundwater from different locations. In winter conditions, extracted groundwater is circulated through a heat exchanger to provide heating in combination with a heat pump. This process reduces the temperature of the extracted water, which is then re-injected into the opposite well at a temperature of 5–10 °C. Under summer conditions, this process is reversed: the cooler water which was injected during the winter is extracted, used for cooling, and re-injected at a temperature of 15–20 °C. Over time, this leads to the formation of warm and cold zones in the groundwater around each well, which should ideally represent equivalent amounts of thermal energy to

maintain the thermal balance of the subsurface. Fig. 1 presents the basic principle of the technology.

The development of these thermal zones is a crucial factor for the performance and management of ATES systems: thermal interferences caused by an insufficient distance between warm and cold wells will lead to energy losses, while neighbouring wells of the same type may have a positive mutual thermal influence. However, the monitoring of these thermal zones is technically challenging, and their evolution is tightly linked to local geohydrological conditions - which are themselves difficult to assess. These characteristics yield significant uncertainties in regards to thermal subsurface dynamics, and therefore to the resulting performance of ATES systems.

These uncertainties are compounded by variable weather conditions and building occupancy patterns, which make it difficult to predict building energy demand and maintain a thermal balance in the subsurface. Actual pumping rates are therefore likely to differ from the expected values which are used for system design and planning; inventories of operational systems also indicate significant year-to-year imbalances between heating and cooling [11]. Persistent imbalances may compromise the long-term viability of ATES development, by changing temperature distributions in the aquifer and potentially affecting the thermal efficiency of systems [12]. Furthermore, imbalances in the thermally-influenced zones around ATES wells are likely to persist over decades or even centuries, due to the low levels of thermal dissipation in the subsurface.

2.2. Management and planning of ATES

Thermal balance and interferences are therefore key elements to consider for the sustainable development of shallow geothermal energy. In response to these issues, management methods for ATES technology have typically followed the precautionary principle [13]. In the Netherlands, revised policies were implemented in July 2013 to reflect new research on the environmental risks of ATES technology; these new policies require permits from provincial authorities for the construction of new ATES systems, which are granted for a given pumping volume on a “first come, first served” basis. Furthermore, design guidelines specify minimal distances between neighbouring wells in order to avoid thermal interactions. These guidelines are based on the average thermal radius R_{th} of the storage wells, i.e. the radius around the wells in which the subsurface temperature is significantly affected; current guidelines specify a conservative distance of $3R_{th}$.

However, these policies take a static view of ATES governance, and do not account for the uncertainties which are inherent to ATES adoption and operation. For instance, permits typically do not incorporate feedbacks from operational performance, which could account for systems being used less than expected; an inventory of 125 ATES systems indicated that less than half the permitted storage capacity was typically used [11]. This gives system operators more flexibility to respond to changes in energy demand or operating conditions, but contributes to the present scarcity of space for further development – as allocated space remains unused.

As an alternative, earlier work [14] summarily evaluated the potential of a self-organized approach for ATES management, which could respond more efficiently to changes in short-term operating conditions, as well as longer-term patterns for the adoption of the technology. Empirical evidence indicates that self-organization – in which cooperative institutional arrangements replace hierarchical planning – may offer an effective alternative for the management of common-pool resources (CPRs)[15]. Considering that the thermal storage potential of the subsurface presents several key features of CPRs [16], self-organization could be appropriate for ATES development due to a relatively small spatial scale, slow resource dynamics, and the high economic benefits of efficient ATES operation [14].

The design of corrective feedbacks and compensation mechanisms will be crucial to preserve the sustainability of the subsurface under such a self-organized approach. This work presents distributed control as a key building block towards a self-organized management regime for ATES; distributed control could support the eventual development of feedback and compensation mechanisms, by providing a framework for the automated exchange of information between ATES users. The case study will test this control approach by first simulating the decoupled, “business-as-usual” operation of ATES systems (hereafter DS), in which individual buildings aim to match the demand and production of thermal energy in the building, while minimizing their operation costs. This is then compared with a distributed multi-agent approach (hereafter DSMPC), which includes information exchange between neighboring buildings to coordinate the operation of their ATES systems, and avoid thermal interferences in the aquifer.

3. Methods

3.1. Model predictive control for ATES systems

Model predictive control (MPC) is a widely used modern optimal control strategy, which typically offers an attractive trade-off between optimality and computational cost. The concept of MPC is simple: predict the behaviour of a system given its model and measurements of the current state of the system, and given a hypothetical control input trajectory or feedback control policy. The control inputs are parameterized by a finite number of variables which denote a finite number of degrees of freedom. The predicted cost of the problem is optimized over these variables, using a given cost function. The control input is then applied to the system in a receding horizon fashion, wherein only the first element of the predicted control input sequence is applied to the system at the current time instant. The horizon is shifted at the next time instant, and the optimization problem is carried out again to obtain a new sequence of control inputs.

The receding horizon strategy is instrumental in reducing the gap between the predicted response and the actual response of the system; this strategy also provides a certain amount of robustness to uncertainty that can arise in the system. This uncertainty arises in the form of uncertain model parameters – which is known as multiplicative model uncertainty – and in the form of additive disturbances appearing from external sources, which is known as additive uncertainty. MPC has the ability to handle operations of processes within well-defined operating constraints, which is not always a given with other methods, but which allows e.g. equipment limits to be represented realistically. These constraints are handled systematically during the design and the implementation of the controller. MPC can respond to structural changes such as actuator and sensor failures, or changes in system parameters, by adapting the control strategy at every time step of execution of the algorithm. For these reasons, MPC has evolved from a basic multivariable process control technology, to a technology that has become widely accepted in industry – which includes the operation of building energy systems and smart thermal grids [17,18]. Compared to conventional methods such as PID controllers, the ability of MPC to handle large-scale dynamical systems under strict constraints offers several advantages for these applications.

3.1.1. Coupling constraints between ATES wells

Ref. [19] presented a MPC formulation for a building climate comfort (BCC) system combining ATES with conventional heating/cooling equipment (i.e. a boiler and chiller). This formulation was first expressed as a finite-horizon, mixed-integer quadratic optimization problem for a single building; as such, this single-agent formulation aims to match the demand and production of thermal energy in the building, while minimizing operation costs and satisfying physical constraints for heating and cooling capacity. This problem was then extended to a centralized multi-agent formulation for multiple buildings. This maintains the individual optimization problems for each building and adds coupling constraints between neighbouring

buildings, in order to avoid mutual interactions between ATES systems.

The coupling constraints rely on the single-agent state variables of the individual ATES systems, which are modelled using first-order difference equations to represent the water volume and thermal energy stored by each building. These equations assume that each ATES system is composed of one warm well and one cold well, which are physically linked; the control variable for the pump flow rate in heating and cooling modes (H and C) is given by $u^H_{a,k}$ and $u^C_{a,k}$ [$m^3\ h^{-1}$] respectively, for each sampling time $k = 1, 2, \ldots$. Taking τ [h] as the sampling period, the usable volume of water stored in the warm and cold ATES wells, V^H_a and V^C_a, is then given by:

$$\begin{aligned} V^H_{a,k+1}\ [\mathrm{m}^3] &= V^H_{a,k} - \tau(u^H_{a,k} - u^C_{a,k}) \\ V^C_{a,k+1}\ [\mathrm{m}^3] &= V^C_{a,k} + \tau(u^H_{a,k} - u^C_{a,k}) \end{aligned} \tag{1}$$

We assume the stored volumes can be approximated by a cylinder with a height equal to the well screen length L [m], following Doughty et al. [20]. Taking a constant aquifer porosity n, this yields hydraulic radii r^H_h, r^C_h for the warm and cold wells:

$$\begin{aligned} r^H_{h,k}\ [\mathrm{m}] &= \sqrt{\frac{V^H_{a,k}}{n\pi L}} \\ r^C_{h,k}\ [\mathrm{m}] &= \sqrt{\frac{V^C_{a,k}}{n\pi L}} \end{aligned} \tag{2}$$

The equivalent thermal radii r^H_{th} and r^C_{th} of the warm and cold wells are then given by:

$$\begin{aligned} r^H_{th,k}\ [\mathrm{m}] &= \sqrt{\frac{c_w V^H_{a,k}}{c_{aq}\pi L}} \\ r^C_{th,k}\ [\mathrm{m}] &= \sqrt{\frac{c_w V^C_{a,k}}{c_{aq}\pi L}} \end{aligned} \tag{3}$$

where c_w and c_{aq} are the specific heat capacity for water and for the aquifer, respectively. For each building agent i, constraints can then be added to the optimization problem in order to avoid overlap between neighboring well radii, so that:

$$(r^H_{th,k})_i + (r^C_{th,k})_j \leqslant \theta d_{i,j}, \quad j \in \mathcal{N}_i \tag{4}$$

where $\mathcal{N}_i$ is the set of neighboring agents of agent i, $d_{i,j}$ [m] is a given distance between wells for agents i and j, and θ is a constant which can be used to adjust the influence of the constraint (so that a larger value will tend to relax the coupling constraint). The coupling constraint can equivalently be applied to hydraulic radii by choosing a different θ parameter.

This formulation assumes that the stored hydraulic and thermal volumes maintain a cylindrical shape in the subsurface, during seasonal pumping patterns as well as displacement by ambient groundwater flow. The validity of this assumption is conditional on well characteristics and aquifer properties; the impact of groundwater flow is evaluated further in appendix, using a dimensionless time-of-travel parameter [21]. In addition, this assumption may not be valid for highly heterogeneous aquifers which present significant variations in hydraulic conductivity. However, for conditions which are typical of effective ATES use, such as the Utrecht area studied in this work, heterogeneity can be expected to have a limited impact on recovery efficiency compared to the effect of ambient groundwater flow or well characteristics [22]. More complex geohydrological conditions will require further study, and may require different coupling formulations.

In parallel, a key requirement for this framework should be its ability to respond to uncertainties in building operation and energy demand. In [19, Problem 21], a suitable multi-agent optimization problem was initially formulated by taking into consideration two possible uncertainty sources, namely, the private (local) uncertainty source, e.g., uncertain thermal energy demand due to the uncertain weather conditions, and the common uncertainty source due to the uncertain common resource pool (ATES) between neighbors. This leads to a finite-horizon, multiple chance-constrained mixed-integer quadratic program, which is in general a non-convex problem and hard to solve. To overcome this difficulty, a tractable framework was developed in [19] in the form of a robust randomized approximation, to obtain a priori probabilistically feasible solutions for each agent. Based on the results presented in [19, Theorem 1], the tractable framework yields solutions which can meet feasibility guarantees at a desired probability threshold, for both local and common uncertain sources, with high confidence levels. This was illustrated by simulating the framework for an idealized building case study with stochastic energy demand, which shows that both the individual building operation constraints, as well as the well coupling constraints, can be suitably met under uncertain exogenous conditions. Such theoretical guarantees can be achieved for any types of uncertainty sources and/or input data, e.g., unknown and unbounded distributions, provided that independent and identically distributed samples of the uncertainties (scenarios) are available.

3.1.2. Distributed control

In practice, the centralized formulation can become computationally too costly to solve for a larger number of agents; in these conditions, distributed control offers improved performance. Distributed MPC aims to replace large-scale centralized optimization problems with several smaller-scale problems, which can be solved in parallel. These problems make use of partial information from other subsystems to implement a distributed solution. In the presence of uncertainties, however, the main challenge in formulating a distributed MPC is the design of a suitable communication scheme to exchange this information between subsystems. Refs. [23,9] provide an appropriate technique to decompose a large-scale scenario-based MPC problem into distributed problems, which exchange a certain number of samples with each other to compute local decisions.

This approach implements the same ATES well coupling constraints as the centralized formulation, using a hierarchical scheme; an upper control layer thus applies the coupling constraints to coordinate the operation of neighboring ATES systems, with weekly time steps and a 3-month prediction horizon. A lower layer then implements the same individual control problem for each building as in [19]. This method can be applied efficiently for larger sets of agents, with computational runtimes scaling $O(n)$ in proportion to the number of agents. This formulation (DSMPC) is therefore used in this work for the ATES simulation study. It is worth highlighting that based on the results presented in [23, Theorem 2], the obtained solutions via the DSMPC framework can meet feasibility guarantees equivalently to the robust randomized approximation discussed in Section 3.1.1. As such, the coupling constraints and building operation constraints remain feasible under stochastic energy demand at a specific level of reliability; as further detailed in [23], this can be theoretically guaranteed provided that appropriate scenario samples are available.

3.2. Coupled building/geohydrological simulation

The simulation study is implemented using a coupled simulation architecture which links a building/control model in MATLAB, an agent-based model of ATES planning in NetLogo [24], and a geohydrological model of groundwater dynamics in MODFLOW/SEAWAT [25,26]. The three model components are linked through an object-oriented Python architecture, so that Python objects form the interface between the three models. Fig. 2 illustrates the basic architecture and shows the data exchanges, which are facilitated by the FloPy pre/post-processor for MODFLOW/SEAWAT [27].

The control formulations for the decoupled and distributed cases are implemented in MATLAB 2016a, using the YALMIP interface [28] with the Gurobi 8.0 solver. The controllers are simulated using given energy demand time series for the building agents, which are generated by a stochastic version of the Low Energy Architecture (LEA) simulation model (detailed in [29]; parameterizations used in this case study are

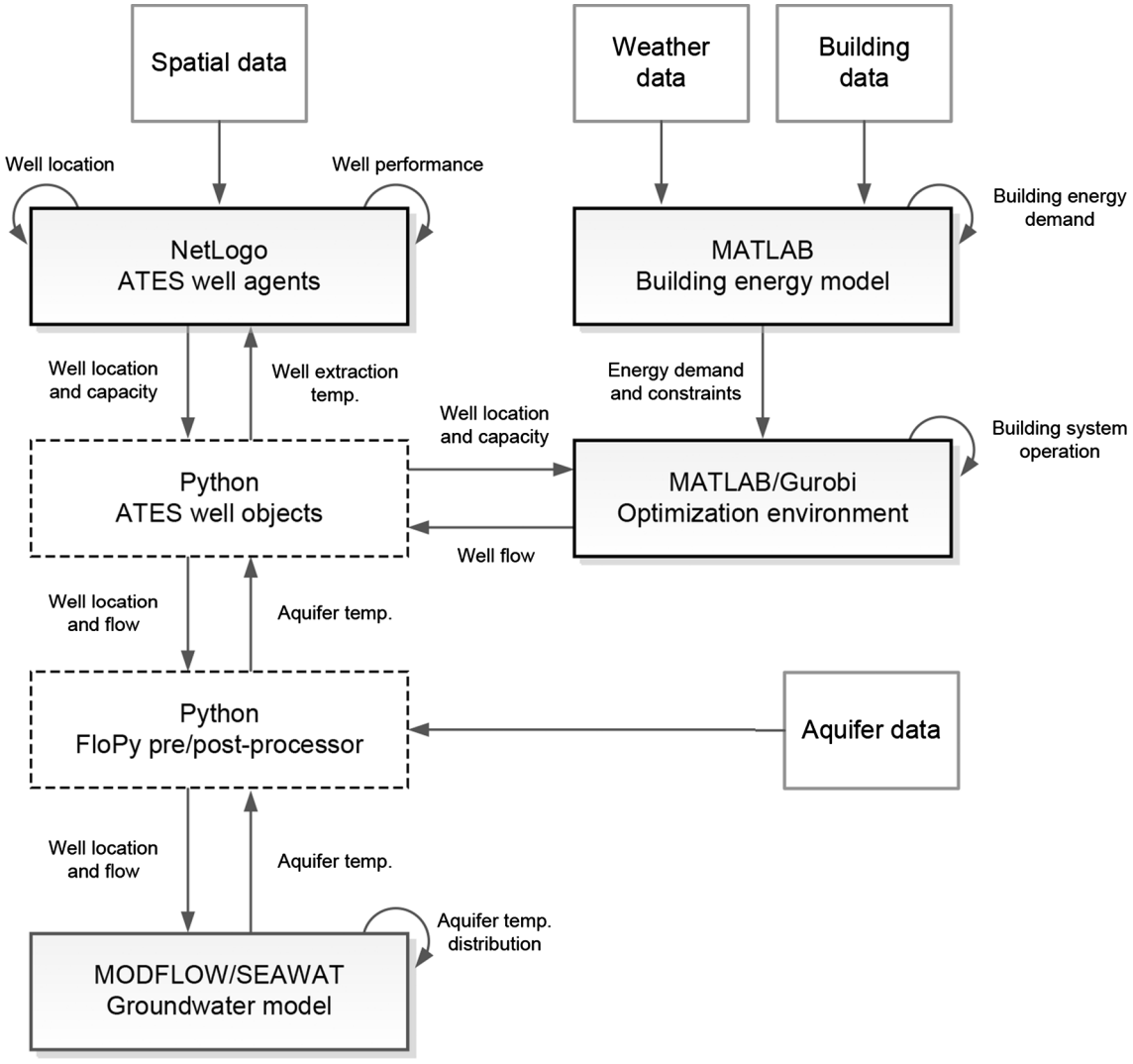

Fig. 2. Simulation architecture.

presented in [30,31]). This energy balance model accounts for weather conditions, building characteristics, and occupancy patterns, and generates the heating and/or cooling demand profiles which are required to maintain a desired indoor temperature. In this application, time series for energy demand, and the corresponding control action for ATES pumping rates of each agent, are computed *ex ante* at an hourly resolution. The ATES pumping rates are then aggregated at a weekly scale and simulated as equivalent ATES well flows in the MODFLOW/SEAWAT groundwater model.

3.2.1. Aquifer properties

The case study uses a 3000 m × 3000 m cutout of the Hydromedah groundwater model for the Utrecht region [32,33]; this model had previously been adapted to include ATES wells, as presented in Bloemendal et al. [34]. As such, the grid is rediscretized in the horizontal plane to refine cells around the ATES wells in each spatial planning scenario, with a grid size varying from 8 m at the center of the wells, to 16 m at the border of the model. The corresponding arrays for horizontal conductivity and groundwater head are rediscretized using bilinear interpolation. The ATES wells are located in a confined layer with an average thickness of 26 m. In addition, the standard MT3DMS packages are parameterized using the assumptions presented in [35], in order to include relevant transport processes.

4. Case study

4.1. ATES performance assessment

The simulation case study uses key performance indicators which build on an earlier assessment framework [5], to evaluate the performance of the DS and DSMPC control methods from the perspectives of ATES system owners and policymakers. For the former, three indicators will be used (with details for the computation of each indicator being presented in appendix):

- The average thermal efficiency of ATES systems (η_{tot}), i.e. the fraction of injected thermal energy which is recovered from the subsurface over a given number of storage cycles;
- The average effective coefficient of performance (COP) of ATES systems, i.e. the ratio between the energy delivered from ATES systems to buildings over a given number of storage cycles, and the energy used to operate the ATES systems;
- The average economic efficiency of ATES systems (νC), defined as specific energy cost savings per unit of water pumped by ATES, relative to a conventional building system delivering the same quantity of heating and cooling energy.

Three additional indicators will be used from the perspective of policymakers:

Table 1
Parameters used for the assessment of the case studies.

Parameter	Value or range	Unit	Symbol
ATES nominal temperature difference	6	[K]	ΔT
ATES pump efficiency	0.3	[–]	η_p
Boiler efficiency	0.9	[–]	COP_b
Chiller coefficient of performance	3	[–]	COP_c
Heat pump coefficient of performance	4	[–]	COP_{hp}
Grid emission factor for electricity	0.157	[tCO_2/GJ]	f_e
Combustion emission factor for natural gas	0.056	[tCO_2/GJ]	f_g
Price for electricity	0.05–0.2	[EUR/kWh]	C_e
Price for natural gas	0.02–0.1	[EUR/kWh]	C_g

- The total GHG savings (Δ_{GHG}) obtained by ATES systems, relative to conventional building energy systems which would deliver equivalent heating and cooling energy;
- The average subsurface usage efficiency of ATES systems (ν_{GHG}), defined as the specific GHG savings obtained per unit of subsurface volume which is allocated for thermal storage;
- The average equivalent GHG abatement cost corresponding to ATES use (α_{GHG}), defined as the ratio between ATES operating costs compared to equivalent conventional building systems, and total GHG savings.

These indicators are computed using the parameters summarized in Table 1, and average over two annual storage cycles.

4.2. Utrecht case

This simulation case study represents a realistic application for the dynamic management of thermal interactions between ATES systems, by (i) testing a DSMPC control formulation which can be scaled to manage ATES thermal interactions across multiple buildings, and (ii) by simulating existing ATES systems and geohydrological conditions in the city center of Utrecht, in the Netherlands. For this case, the building/control models are configured to represent operational uncertainties through a variable demand for ATES storage; due to computational limitations, stochastic uncertainty in building energy demand is not considered, but previous work showed that the control formulations can suitably respond to variable energy demand [23]. The effective maximum storage capacity of ATES systems is here set by applying a multiplier Q to the nominal permitted storage capacity, with $0.6 \leqslant Q \leqslant 1.1$ to match typical operational conditions [11].

Three spatial planning scenarios are used to compare different pathways for the future development of ATES in the area. Following an earlier case study [34], these scenarios assume that ATES wells are built on 9 building plots on which ATES is currently used in the area, starting from a set of 82 currently active or planned wells. The NetLogo agent-based model is used to locate additional simulated ATES wells in a 2000 m × 2500 m grid, on which GIS data is overlaid to generate exclusion areas corresponding to roads, buildings, and waterways. The storage capacity of each additional simulated ATES well is randomly picked from a distribution obtained from a dataset of the permitted capacity of existing ATES systems in the Netherlands, as described in [5].

Scenario 1 represents future development under current layout guidelines in the Netherlands (i.e. well distances of 3.0 R_{th}). Scenarios 2 and 3 then simulate revised, denser layout guidelines of 2.5 R_{th} and 2.25 R_{th}, respectively. In all scenarios, simulated new wells are located in available development areas, as long as sufficient space is available under the layout guidelines. These scenarios are illustrated in Fig. 3. The dashed lines between wells illustrate the "coupling" constraints for the DSMPC formulation, which aim to avoid interferences between neighboring wells. These constraints are in this case applied to wells of

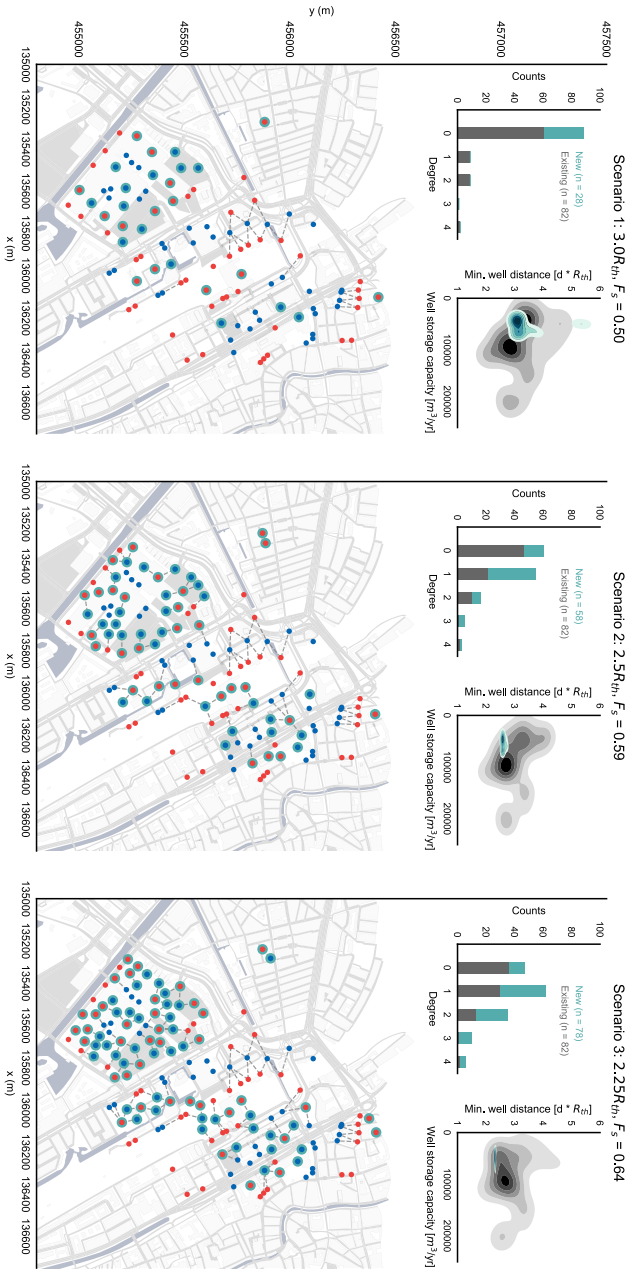

Fig. 3. Spatial planning scenarios for Utrecht case study. Dashed lines indicate constrained well pairs; outlined markers indicate existing or planned ATES wells.

opposite types (i.e. warm/cold) with a relative distance below 2.75 R_{th}. This distance approximately represents the maximum distance at which thermal interactions can be expected to be significant [5].

Inset plots show a bivariate Gaussian kernel density estimate for the distribution of nominal well capacities in each scenario (distinguishing between existing or planned wells, and simulated new wells), and for the distribution of the minimum relative distance to any neighboring well. For instance, this indicates that the simulated new wells in all scenarios have capacities below 100,000 m^3/year, as there is already a lack of space to accommodate larger wells on existing building plots. In parallel, the new wells built in Scenario 3 all have minimum distances of approximately 2.25 R_{th} with other wells, while the sparser guidelines in Scenario 1 lead to a broader distribution on this indicator; we can for instance expect that wells which are not within 3.0 R_{th} of other wells would not be significantly affected by the dynamic management of

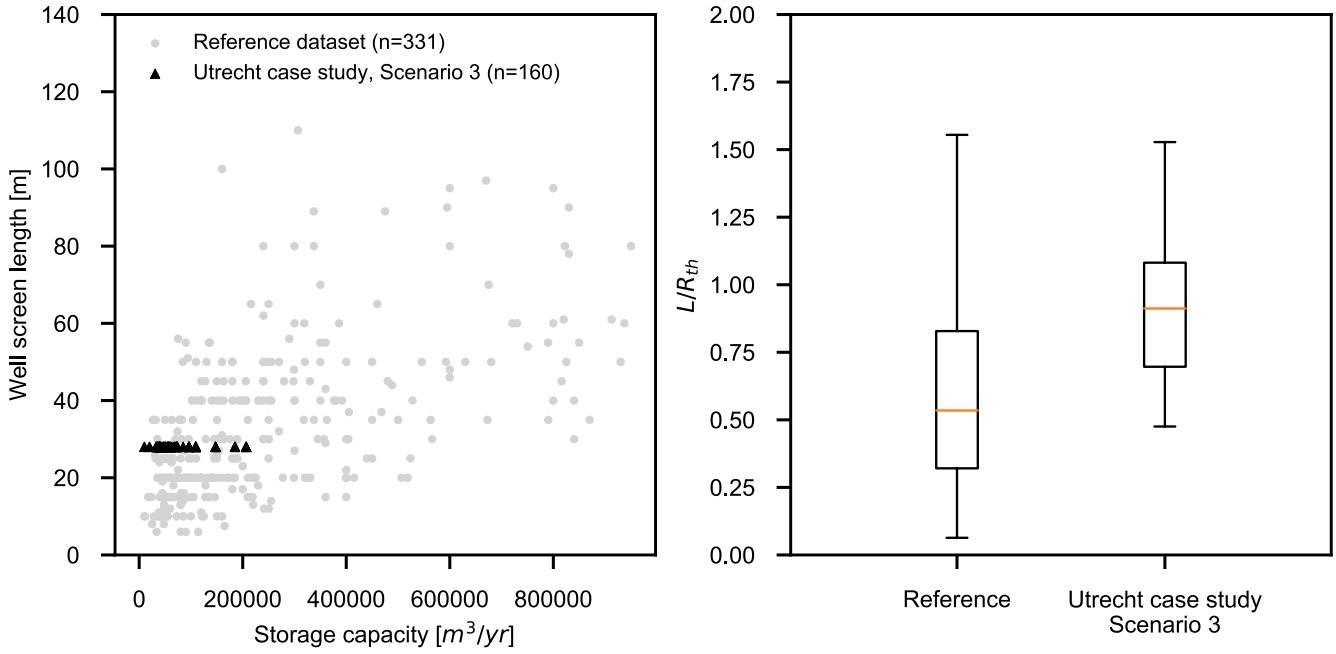

Fig. 4. Well characteristics as simulated in the idealized case study and Utrecht case study, compared to the reference dataset used in Bloemendal and Hartog [35]. Left panel: well screen length vs. nominal storage capacity; right panel: distribution of the L/R_{th} ratio across the wells in each sample.

thermal interactions.

Given that the simulated new wells in Scenarios 2 and 3 are located under different layout guidelines than the existing or planned wells, the management of thermal interactions is likely to impact these groups of wells in different ways – potentially leading to a different distribution of benefits across incumbent ATES users and new adopters. The case study will thus use a simple game-theoretical approach, to test the combinations of ATES usage and energy prices under which cooperation (i.e. participation in an information exchange scheme) would be a Pareto-optimal Nash equilibrium. This analysis assumes that the ATES wells are grouped into "incumbent" and "new" systems.

In order to place these scenarios in the context of typical conditions for ATES in the Netherlands, Fig. 4 compares the characteristics used in the case study with a dataset of 331 Dutch ATES wells studied by Bloemendal and Hartog [35]. As shown in the left panel, the simulated wells tend to be relatively small, in terms of annual storage capacity as well as screen length; the right panel presents the distribution of the ratio between the well screen length and thermal radius (L/R_{th}). This ratio has a significant impact on thermal efficiency [20], and has additional implications in the context of a DSMPC approach: the dynamic management of thermal interactions is likely to be more useful with smaller L/R_{th} values, which relatively increase the horizontal footprint of the wells. In these conditions, the magnitude of the changes in stored radii through direct transport (which can be directly controlled) would be relatively greater in relation to the magnitude of conduction and dispersion processes between the stored thermal volume, and the ambient aquifer medium (which are largely uncontrolled, and driven by aquifer properties). As the Utrecht sample has relatively high values on this indicator compared to typical practices, the case study should therefore offer a conservative example of interaction management, with other areas potentially being better suited for this approach.

5. Results

5.1. System performance and distributional effects

Fig. 5 presents the average system performance indicators for each spatial planning scenario, as a function of the total volume of water pumped by ATES systems. The DS formulation yields a consistent trend, in which performance tends to decrease within each planning scenario (i.e. with an increase in the allowed pumped fraction Q), and across the planning scenarios (i.e. with an increase in well density). In parallel, the total pumped volume of water increases in proportion to the allowed pumped fraction Q, as expected.

The DSMPC formulation presents significantly different behavior: the total pumped volume of water tends to saturate at $Q = 1.0$, then drops for $Q = 1.1$. This is accompanied by an improvement in the system performance indicators. This behavior is explained by the decrease in usage of wells which are subject to multiple coupling constraints with neighboring wells, and which typically have a lower thermal efficiency due to this density; with an increase in allowed pumped capacity, these "marginal" wells tend to be used less in order to meet the coupling constraints – thus increasing average performance. Fig. A.11 in appendix details this effect, by plotting the relative usage of the well pairs simulated in Scenario 3, as a function of their decoupled thermal efficiency. Less efficient wells thus tend to be used less when applying the coupling constraints.

For values of $Q = 1.0$, the performance of the systems typically remains at least equal to performance at $Q = 0.6$; Table A.2 summarizes these results, computed as "regret" values relative to the DS formulation in Scenario 1 (i.e. $R_{th} = 3.0$).

However, assumptions on energy prices may further complicate the situation; economic performance does not always exactly correlate with thermal efficiency, depending on the relative costs of energy for heating or cooling. As such, whereas high gas prices directly increase cost savings from ATES relative to a conventional boiler, electricity prices have a more complex effect, by affecting the operating cost of ATES well pumps and the building heat pump, as well as cost savings relative to a conventional chiller. Fig. 6 presents the relative economic performance of different control/layout combinations, based on the specific energy cost savings per unit of water pumped by ATES in each case. For Scenario 3, this implies that the DSMPC formulation would outperform the DS formulation across all tested energy price combinations, which are based on typical non-household energy prices for electricity and natural gas in the European Union [36,37]). However, energy price combinations which tend to make ATES more relatively profitable overall (i.e. high gas prices and low electricity prices) would slightly penalize the relative performance of the DSMPC/Scenario 3

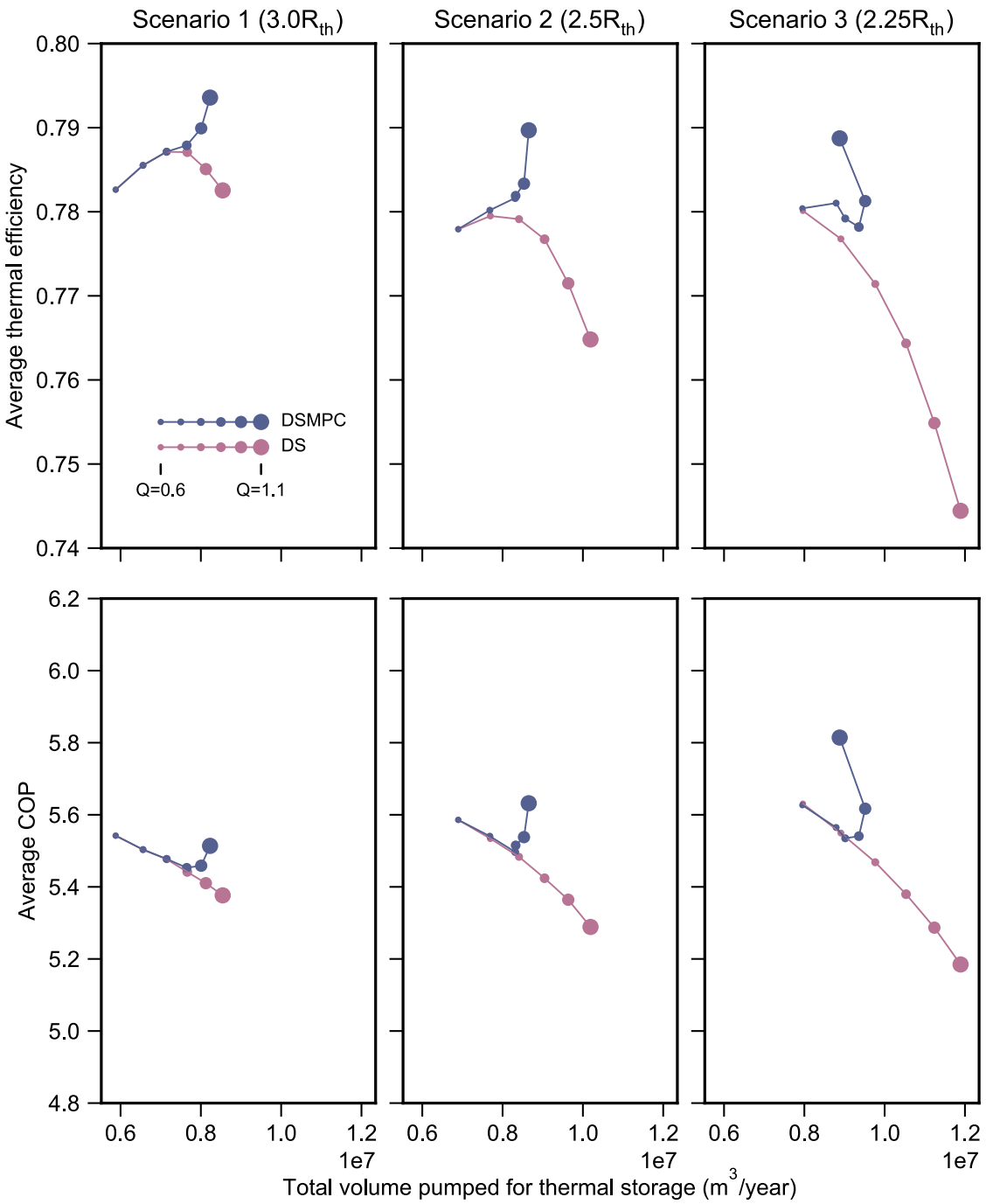

Fig. 5. ATES performance indicators for Utrecht case, for each spatial planning scenario: average thermal efficiency (top panel) and coefficient of performance (bottom panel).

combination, compared to "business-as-usual" development (DS, Scenario 1). Notably, in conditions where ATES would be less profitable overall, the DSMPC formulation retains a relative advantage due to more efficient pumping schedules.

The analysis has so far considered average results over the full set of active wells. However, Scenarios 2 and 3 in particular may lead to different benefits for existing (or "incumbent") wells, and simulated wells created under different layout guidelines. In this situation, new and incumbent wells may decide to partially cooperate, i.e. to exchange information across their subset of wells only. To evaluate the conditions under which these two groups of users could be assumed to have an incentive to cooperate in exchanging information, Figs. 7 and 8 present the effect of different plausible combinations of energy prices and Q values, on the average cost savings of each group of users for Scenario 3. The markers present four possible courses of action: *full cooperation* (i.e. the DSMPC formulation), *only incumbent wells coupled*, *only new wells coupled*, and *no cooperation* (i.e. the DS formulation). The energy cost savings for each action are then considered as payoffs in a 2-player game; shaded subplots indicate that full cooperation is not a Nash equilibrium in a given combination.

Fig. 7 thus indicates that relatively high electricity prices may prevent cooperation from being a Nash equilibrium, when combined with a lower ATES usage ($Q = 0.7$) and low gas prices; this combination makes ATES relatively less economically attractive. In this situation, incumbent wells would benefit from full cooperation, while the Pareto-optimal decision for new wells would be to only partially cooperate

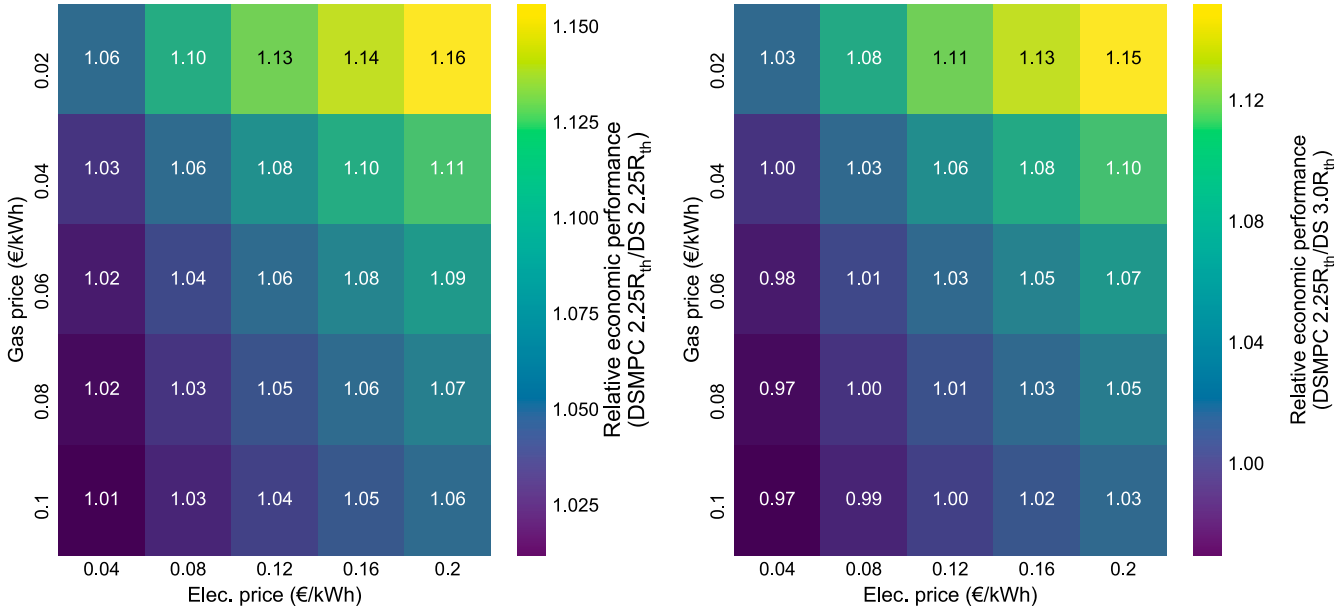

Fig. 6. Relative economic performance across different control/layout combinations. Left panel: DSMPC compared to DS, for Scenario 3 ($2.25R_{th}$). Right panel: DSMPC for Scenario 3, compared to DS for Scenario 1.

within their own subset.

However, for $Q \geqslant 1.0$, the greater overall cost savings from a larger usage of ATES then yield a cooperative Nash equilibrium in all of the energy price combinations, as illustrated in Fig. 8.

5.2. Collective performance

Given that GHG savings are largely driven by the total pumped volume, a similar pattern holds for the GHG indicators shown in Fig. 9 as for system performance. As such, in the DS formulation, the value of both indicators increases monotonically with the allowed pumped fraction Q, but reaches a maximum at $Q = 1.0$ for the DSMPC case.

As indicated in the tabular results shown in appendix, the increase in specific GHG savings is significant for denser layout guidelines (e.g. 37% with the DSMPC formulation in Scenario 3). The highest specific GHG savings are obtained with the DS formulation in Scenario 3, which maximizes the total pumped water volume; however, the associated decrease in system performance would likely be unacceptable for ATES owners.

This trade-off can be expressed through the equivalent marginal GHG abatement cost, which relates energy cost savings and GHG savings. The left panel of Fig. 10 presents the GHG abatement cost for the DSMPC formulation in Scenario 3; the negative values indicate that the additional development of ATES systems allowed in this case would nonetheless be economically attractive compared to conventional energy. In parallel, the right panel presents the marginal GHG abatement cost which is obtained by comparing the DSMPC formulation in Scenario 3, with the "business-as-usual" case (DS, Scenario 1). As previously shown in Fig. 6, a higher gas price combined with a relatively lower electricity price tends to make the DSMPC approach relatively less economically attractive. However, considering the overall improvements in GHG savings which would be supported by this approach, the equivalent GHG abatement cost is relatively low; this cost is for instance below typical carbon prices for the European Union Emissions Trading System for the 2017–2018 period.

Under the assumptions used to parameterize the models, this implies that denser ATES development with a DSMPC approach would remain an economically attractive GHG abatement option for policymakers, even under an unfavorable combination of energy prices. Furthermore, the opposite combination of energy prices (i.e. low gas price and high electricity price, which tends to make ATES more economically sensitive to pumping schedules) would favor the DSMPC approach, yielding negative marginal abatement costs.

6. Discussion and conclusions

Current methods for the planning and operation of ATES systems lead to an inefficient trade-off between private and public interests, by limiting the deployment of the technology – and thus energy savings – in the dense urban areas which account for a growing portion of energy use in the built environment. This situation is motivated by the risk of a "tragedy of the commons" which could be caused by uncontrolled thermal interferences between ATES systems sharing an aquifer. As a starting point towards an improved management regime which could resolve this trade-off, this work assessed an approach based on the distributed control of ATES systems, in which information exchange would support the dynamic management of thermal interactions between neighboring ATES systems. Based on the results of a simulation case study for the city center of Utrecht, in The Netherlands, this approach could significantly improve greenhouse gas savings from ATES, without compromising the performance of individual systems. Compared to a "business-as-usual" case, information exchange – combined with a denser layout policy for ATES wells – respectively yielded improvements of 21% and 38% in total GHG savings and specific GHG savings per unit of allocated subsurface volume, at a comparable average level of economic performance.

A coordinated approach to ATES operation could thus change the structure of the trade-off between private and public interests: under plausible operating conditions, the exchange of information across ATES systems could lead to a "win-win" situation for policymakers and operators, by increasing collective GHG savings without penalizing economic performance. However, this approach would lead to a different compromise, under which ATES operators would trade off the implicit value of information about their use of ATES and other building energy systems. The privacy implications of smart energy systems have drawn increased scrutiny in the literature [38]; in the case of industrial energy users, thermal demand profiles could for instance be used to infer sensitive information about production processes [39]. Similarly, in the case of residential users, aggregation across multiple sources and levels of energy usage may make it impossible for participating

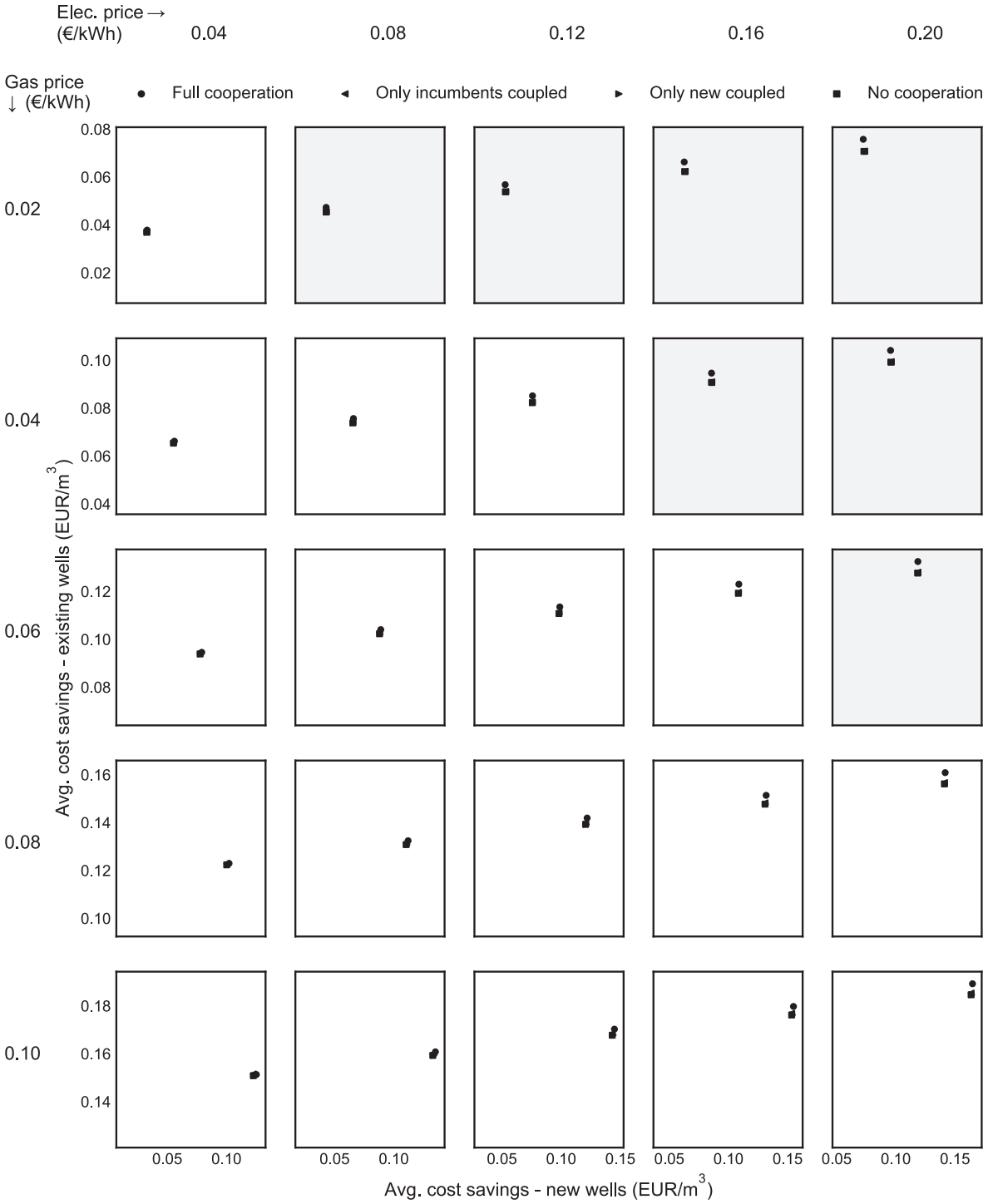

Fig. 7. Game-theoretical analysis for cooperation between incumbent and new wells, as a function of gas and electricity prices, for $Q = 0.7$ and Scenario 3. Shaded subplots indicate that full cooperation is not a Nash equilibrium in a given combination of energy prices.

individuals to offer genuinely informed consent towards the use of their data [38]. Although dedicated research is needed to assess these issues in the specific context of ATES, we note that the DSMPC approach is entirely compatible with differential privacy methods, under which the required information is pre-processed to maintain a level of privacy for the participating agents [40]. This would then entail a trade-off between the bandwidth of exchanged information, and its reliability towards the management of thermal interactions.

We emphasize that taking advantage of the dynamic management of thermal interactions will also require revised spatial planning policies: the current guidelines used to plan ATES systems in the Netherlands are effective at avoiding thermal interactions between systems, which implies there would be little benefit in their management. This was supported by the results of the simulated case study, in which a coordinated approach showed limited gains under current ATES well layout guidelines of $3.0R_{th}$. In parallel, a comparison of the spatial planning scenarios with a larger dataset showed that the Utrecht case study was generally representative of typical conditions in the Netherlands, but that the simulated wells presented relatively high values for the ratio between well screen length and thermal radius

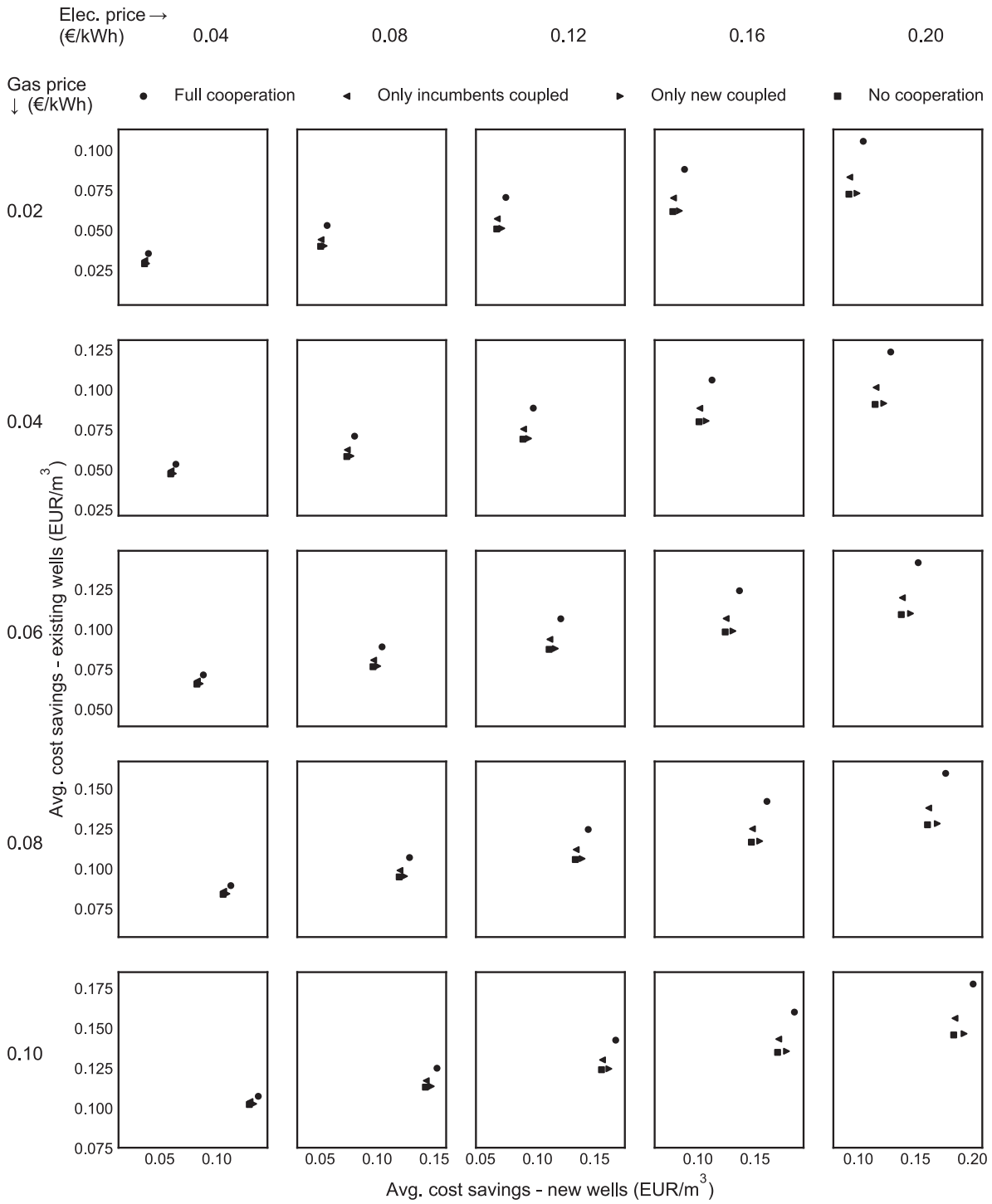

Fig. 8. Game-theoretical analysis for cooperation between incumbent and new wells, as a function of gas and electricity prices, for $Q = 1.1$ and Scenario 3.

(L/R_{th}). The dynamic management of thermal interactions is likely to offer additional benefits with smaller L/R_{th} values, e.g. with relatively shorter well screen lengths and shallower aquifers. In these conditions – and with the assumption of a cylindrical storage volume – seasonal pumping patterns will intuitively yield larger variations in the radii of storage wells. The dynamic management of these radii through well coupling constraints would in turn allow for more precise management of thermal interactions between neighboring thermal volumes. Due to the relatively larger resulting footprint of wells in the horizontal plane, shallower aquifers are also more likely to experience a scarcity of space for new ATES systems, making the management of interactions particularly relevant in these cases. This case study should therefore be relatively conservative in regards to the benefits of distributed ATES control.

Due to computational limitations, the case study only tested a limited number of scenarios for spatial planning and building operating conditions. However, earlier theoretical work on the development of the control formulation used in this work [19,23] showed that the formulation can suitably respond to changes in building energy demand and other exogenous drivers, so that the well coupling constraints would be robust to operational uncertainties. The formulations could for instance be further developed in this regard by explicitly accounting

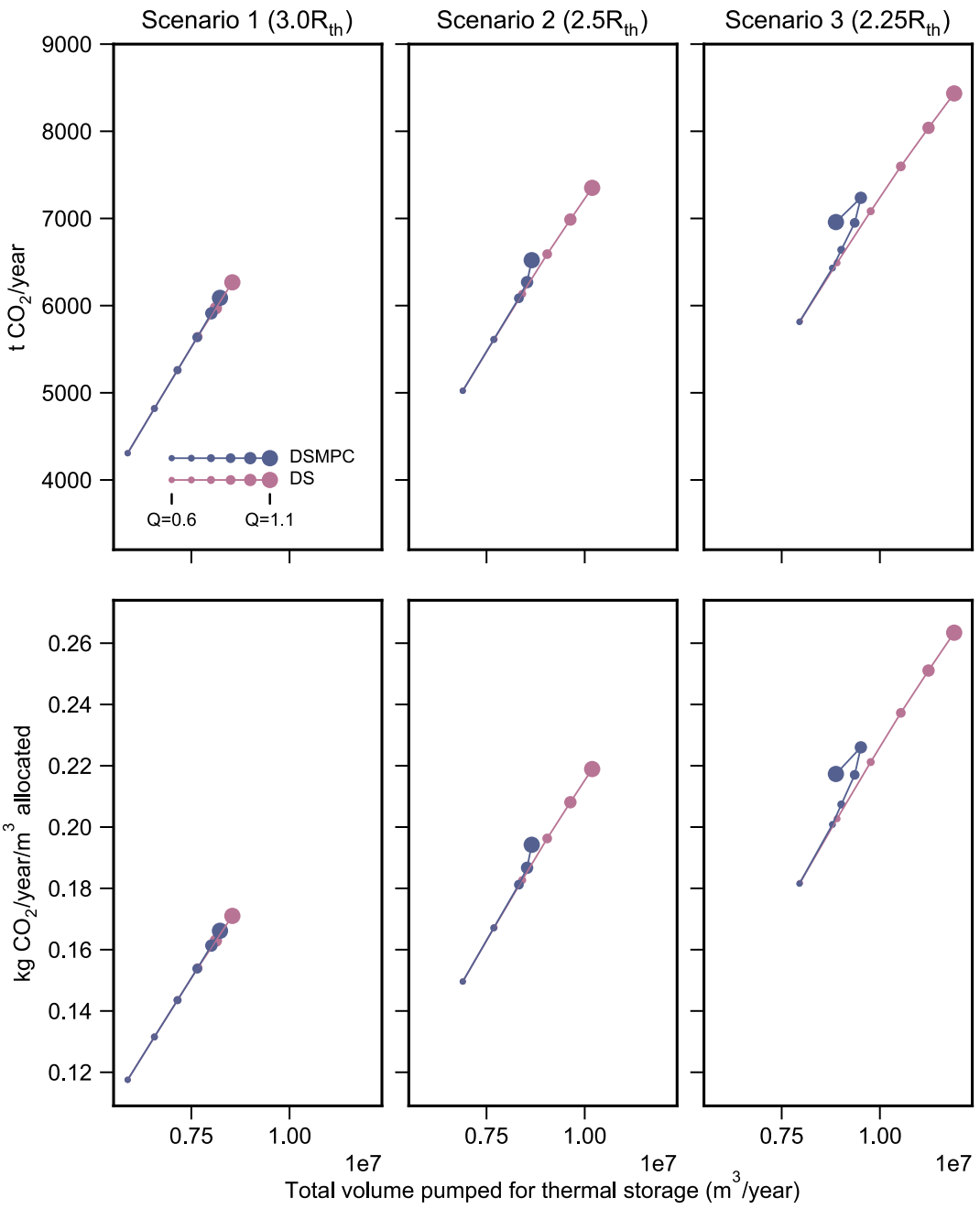

Fig. 9. Collective performance indicators for Utrecht case, for each spatial planning scenario: total annual GHG savings (top panels); specific annual GHG savings per allocated unit of subsurface volume (bottom panels).

for ambient groundwater flows.

Finally, we note that the current rapid deployment of ATES provides a window of opportunity to apply such improved methods for the planning and operation of systems, as policymakers and ATES operators may otherwise become locked into suboptimal practices. As such, the next steps for this research will focus on interfacing the ATES control formulation with an existing building system model, which will enable the controller to be tested in more realistic conditions and bring this approach closer to practice.

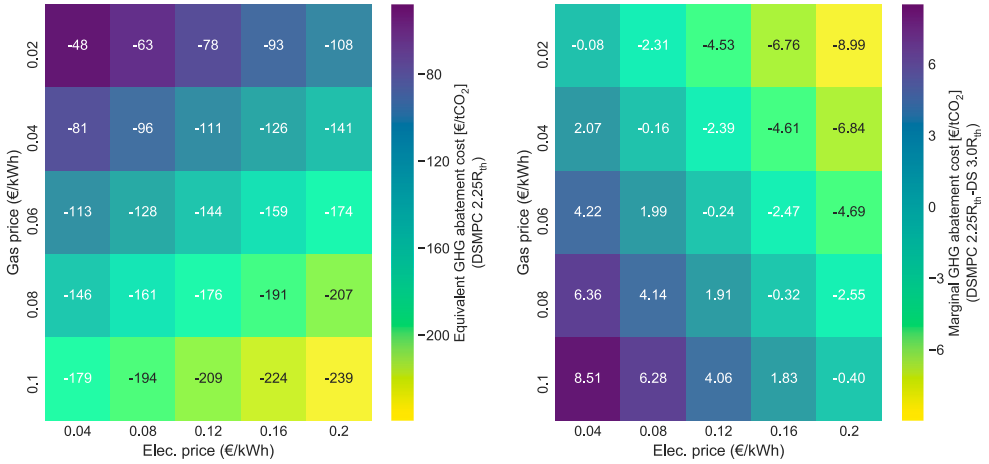

Fig. 10. Left panel: equivalent GHG abatement cost for DSMPC in Scenario 3 ($2.25R_{th}$). Right panel: marginal GHG abatement cost for DSMPC in Scenario 3, compared to "business-as-usual" development (DS, Scenario 1).

Appendix A. Assessment framework

The following framework builds on Bloemendal et al. [5].

A.1. Energy use and emissions of ATES systems

The energy balance of the heat pump is used to trace back the heating and cooling demand (E_h, E_c) of the associated buildings and the energy consumption by the heat pump. The total heating capacity for the building provided by the heat pump is described by two basic relations:

$$P_h = P_{ATES} + P_e \quad \& \quad COP_{hp} = \frac{P_h}{P_e} \tag{A.1}$$

where P_h [W] is the heating capacity deliverable to the building; P_{ATES} [W] the thermal heating power retrieved from the groundwater, P_e [W] the electrical power consumed by the heat pump and COP_{hp} coefficient of performance of the heat pump. Eq. (A.1) shows that all electric power fed to the heat pump contribute to the heat output. When it is assumed that 100% of the heating and cooling demand of the building is delivered by the ATES system, the heating capacity and total heat energy ($E_{h,ATES}$) from the groundwater between times t and t_0 equals

Table A.2
Performance values for Utrecht case study with $Q = 1.0$, relative to DS Scenario 1.

	Scenario 1 (3.0 Rth)		Scenario 2 (2.5 Rth)		Scenario 3 (2.25 Rth)	
	DSMPC	DS	DSMPC	DS	DSMPC	DS
Thermal efficiency	1.007	1.0	1.001	0.971	0.998	0.941
COP	1.010	1.0	1.015	0.968	1.034	0.949
Total GHG savings	0.990	1.0	1.060	1.159	1.212	1.290
Specific GHG savings	0.990	1.0	1.157	1.265	1.388	1.518

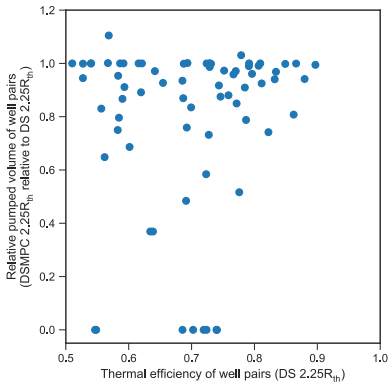

Fig. A.11. Effect of well coupling constraints on pumped volume for Utrecht case study, as a function of decoupled thermal efficiency in Scenario 3. Each of the markers corresponds to a simulated well pair.

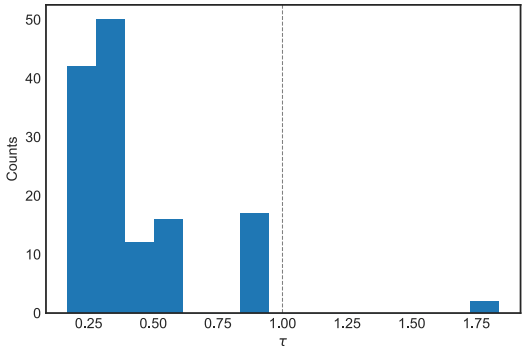

Fig. A.12. Distribution of the dimensionless time-of-travel parameter τ across the wells simulated for Scenario 3 of the Utrecht case study. Values below 1 imply an approximately cylindrical capture zone.

$$E_{h,ATES}\left(t_0 \rightarrow t\right) = c_w \int_{t_0}^{t} P_{ATES}\, dt \tag{A.2a}$$

$$= c_w \Delta \bar{T}_h \int_{t_0}^{t} Q dt \tag{A.2b}$$

$$= c_w \Delta \bar{T}_h V_h \tag{A.2c}$$

with

$$P_{ATES} = c_w Q (T_w T_c) = c_w Q \Delta T_h \tag{A.3}$$

The integration is done for the whole heating season ($t_0 \rightarrow t$). V_h [m^3] is the given seasonal volume of groundwater required for heating. ΔT [K] is the instantaneous temperature difference between the warm (T_w) and cold (T_c) well, is the average temperature difference during heating season, Q [m^3/h] is the groundwater flow from the warm well to the cold well and c_w [J/m^3)/K] is the volumetric heat capacity of the water. With V_h substituted in Eqs. (A.1) and (A.3), Eq. (A.4) yields the heat E_h [J] delivered to the building over the heating season:

$$E_h = c_w \Delta \bar{T}_h V_h \frac{COP_{hp}}{COP_{hp} - 1} \tag{A.4}$$

The cooling delivered to the building is calculated using the same equations, while distinguishing between free cooling and heat pump cooling. An absolute temperature threshold of 9 °C was set for the cold well above which no free cooling is assumed possible. When the extraction temperature of the cold well surpasses this threshold, the heat pump is used to meet the cooling demand and resulting heat is transferred to the warm well via the condenser of the heat pump. The total cooling delivered to the building then follows from:

$$E_c = c_w \Delta \overline{T}_{c,fc} V_{c,fc} + c_w \Delta \overline{T}_{c,hp} V_{c,hp} \frac{COP_{hp} - 1}{COP_{hp} - 2} \tag{A.5}$$

in which $V_{c,fc}$ and $V_{c,hp}$ are the groundwater volumes required for free cooling and cooling by the heat pump and $\Delta T_{c,fc}$ and $\Delta T_{c,hp}$ are the average temperature differences between the warm and cold well for free cooling and cooling by the heat pump respectively. Note that the heat pump COP is 1 lower during cooling. The total energy consumption of the ATES system (E_{ATES}) is completed by including the pump energy consumption. Substituting Eqs. (A.1) into (A.4) and (A.5) yields:

$$E_{ATES} = \frac{E_h}{COP_{hp} - 1} + \frac{E_{c,hp}}{COP_{hp} - 2} + \frac{(V_h + V_{c,fc} + V_{c,hp})\Delta p}{\eta_p} \tag{A.6}$$

where Δp is the lifting pressure generated by the groundwater pump and η_p its nominal efficiency. The effective coefficient of performance of the ATES systems corresponds to the ratio between the quantities of energy which are delivered and used:

$$COP = \frac{E_h + Ec}{E_{ATES}} \tag{A.7}$$

In parallel, the energy efficiency (η) of a well over the simulation period is calculated in weekly steps by dividing the extracted amount of thermal energy by the infiltrated amount of thermal energy. The thermal efficiency taken over all the wells in the model (η_{tot}) is the average of the individual efficiencies, weighted by the individual total storage volume of the wells ($V_i = V_{h,i} + V_{c,fc,i} + V_{c,hp,i}$)

$$\eta_{tot} = \frac{\sum_{i=1}^{n} \eta_i V_i}{\sum_{i=1}^{n} V_i} \tag{A.8}$$

The equivalent GHG emissions [tCO_2] are retrieved by calculating the CO_2 emissions of the considered ATES systems:

$$GHG_{ATES} = \sum_{i=1}^{n} E_{ATES,i} f_e \tag{A.9}$$

where f_e [tCO_2/GJ] is the grid emission factor for electricity, E_{ATES} [GJ] is the electricity consumption of the ATES system, and n the number of active ATES wells. The calculation assumes a representative emissions factor for delivered electricity in the Netherlands.

A.2. Energy use and emissions of reference boiler/chiller systems

As a reference for technical and economic performance of ATES systems, the calculation considers a conventional climate control installation which would deliver the same amount of heating E_h [GJ] and cooling energy E_c [GJ] to the building. It is assumed that natural gas is used for heating in a boiler with combustion efficiency COP_b, and that electricity is used for a cooling machine operating at a constant coefficient of performance COP_c. The energy consumption and greenhouse gas emissions [tCO_2] for these buildings then equal:

$$E_{boiler} = \frac{E_h}{COP_b} \quad \& \quad E_{chiller} = \frac{E_c}{COP_c} \tag{A.10}$$

$$GHG_{conv} = \sum_{j=1}^{n} \left(E_{boiler,j} f_g + E_{chiller,j} f_e \right) \tag{A.11}$$

in which f_e [tCO_2/GJ] is the emission factor for gas and m the number of active conventional systems (which we here consider to be equal to the number of ATES systems).

A.3. Economic parameters

Operational costs for ATES and conventional systems can be computed similarly to GHG emissions, using the electricity price C_e [EUR/GJ] and natural gas price C_g [EUR/GJ] instead of the emission factors:

$$C_{ATES} = \sum_{i=1}^{n} E_{ATES,i} C_e \tag{A.12}$$

$$C_{conv} = \sum_{j=1}^{n} \left(E_{boiler,j} C_g + E_{chiller,j} C_e \right) \tag{A.13}$$

The economic efficiency of ATES can then be expressed as cost savings per total volume of water used for storage [EUR/m^3]:

$$\nu C = \frac{C_{conv} - C_{ATES}}{\sum_{i=1}^{n} V_{h,i} + V_{c,fc,i} + V_{c,hp,i}} \tag{A.14}$$

We note that this analysis focuses on operational costs only rather than upfront investment costs, given the high variability of fixed costs for ATES across different sites and buildings [6].

A.4. Collective performance indicators

The simulated GHG savings Δ_{GHG} [tCO_2] correspond to the difference between the emissions of conventional energy systems and ATES systems, for a given amount of delivered energy:

$$\Delta_{GHG} = GHG_{conv} - GHG_{ATES} \tag{A.15}$$

As a measure of the efficiency with which subsurface volume is used for thermal storage, these greenhouse gas savings can be expressed in relation to the aquifer volume allocated to ATES wells, using the distance policy d, well screen length L_i [m] and the total nominal storage volume of the wells V_i [m^3/yr]:

$$\nu_{GHG} = \frac{\Delta_{GHG}}{\sum_{i=1}^{n} \pi d R_{th,i}^2} = \frac{c_{aq}}{c_w} \frac{\Delta_{GHG}}{\sum_{i=1}^{n} \frac{V_i}{L_i}} \tag{A.16}$$

Finally, cost savings and GHG savings can be related as an equivalent GHG abatement cost α_{GHG} [EUR/tCO_2], which will be negative if cost and GHG savings from ATES are both positive:

$$\alpha_{GHG} = (C_{ATES} - C_{conv})/\Delta_{GHG} \tag{A.17}$$

Appendix B. Supplementary results

See Table A.2 and Fig. A.11.

Appendix C. Impact of aquifer conditions on thermal recovery

The formulation of the well couplings assumes that the stored hydraulic/thermal volumes of each ATES well can be described by a cylindrical shape, following Doughty et al. [20]. In practice, ambient groundwater flow may cause significant changes in the effective (i.e. recoverable) shape of the stored volumes. As such, to justify the assumption of a cylindrical recoverable volume, we use a dimensionless time-of-travel parameter, for which values smaller than 1 imply a circular (but possibly eccentric) capture zone around each well [21]:

$$\tau = \frac{2\pi (ik)^2 L t_{sp}}{nQ} \tag{A.18}$$

This parameter is based on the groundwater head gradient i, hydraulic conductivity k, screen length L, storage period t_{sp}, aquifer porosity n, and stored volume Q. Using the parameters of the wells simulated in Scenario 3 of the Utrecht case study as well as the simulated aquifer properties, Fig.

A.12 presents the resulting distribution of the value of τ across all simulated wells. This assumes an average seasonal storage period of half a year.

As such, only two wells would not meet the assumption of a cylindrical capture zone, due to their relatively small capacity relative to the ambient groundwater flow. In addition, heat transfer to the aquifer medium will delay the transport of heat relative to the groundwater flow, by a factor of approximately two [35]. The assumption of a cylindrical capture zone should therefore offer a reasonably accurate approximation; the choice of the coupling scaling parameter θ can be used to compensate the impact of eccentric capture zones on thermal interactions. Further work could explicitly add a groundwater flow term to the formulation of the well couplings, in order to increase the accuracy of the couplings under higher ambient flow values.

References

[1] Vanhoudt D, Desmedt J, Van Bael J, Robeyn N, Hoes H. An aquifer thermal storage system in a Belgian hospital: long-term experimental evaluation of energy and cost savings. Energy Build 2011;43(12):3657–65. https://doi.org/10.1016/j.enbuild.2011.09.040.

[2] Fleuchaus P, Godschalk B, Stober I, Blum P. Worldwide application of aquifer thermal energy storage–a review. Renew Sustain Energy Rev 2018;94:861–76.

[3] Bloemendal M, Olsthoorn T, van de Ven F. Combining climatic and geo-hydrological preconditions as a method to determine world potential for aquifer thermal energy storage. Sci Total Environ 2015;538:621–33. https://doi.org/10.1016/j.scitotenv.2015.07.084.

[4] Hardin G. The Tragedy of the Commons. Science 1968;162(3859):1243–8. https://doi.org/10.1126/science.162.3859.1243.

[5] Bloemendal M, Jaxa-Rozen M, Olsthoorn T. Methods for planning of ATES systems. Appl Energy 2018;216:534–57. https://doi.org/10.1016/j.apenergy.2018.02.068.

[6] Agterberg F. Developing strategic options for the Dutch subsoil energy sector Master's thesis TIAS School for Business and Society; 2016.

[7] Sommer W, Valstar J, Leusbrock I, Grotenhuis T, Rijnaarts H. Optimization and spatial pattern of large-scale aquifer thermal energy storage. Appl Energy 2015;137(2015):322–37.

[8] Pophillat W, Attard G, Bayer P, Hecht-Méndez J, Blum P. Analytical solutions for predicting thermal plumes of groundwater heat pump systems. Renew Energy. https://doi.org/10.1016/j.renene.2018.07.148.

[9] Rostampour V, Keviczky T. Distributed stochastic model predictive control synthesis for large-scale uncertain linear system with private and common uncertainty sources. arXiv preprint arXiv:1703.06273.

[10] Bayer P, Saner D, Bolay S, Rybach L, Blum P. Greenhouse gas emission savings of ground source heat pump systems in Europe: a review. Renew Sustain Energy Rev 2012;16(2):1256–67. https://doi.org/10.1016/j.rser.2011.09.027.

[11] Willemsen N. Rapportage bodemenergiesystemen in Nederland,. Tech. rep., RVO/IF Technology, Arnhem, The Netherlands; 2016.

[12] Calje R. Future use of aquifer thermal energy storage below the historic centre of Amsterdam Master's thesis Delft University of Technology; 2010.

[13] Hähnlein S, Bayer P, Ferguson G, Blum P. Sustainability and policy for the thermal use of shallow geothermal energy. Energy Policy 2013;59:914–25. https://doi.org/10.1016/j.enpol.2013.04.040.

[14] Bloemendal M, Olsthoorn T, Boons F. How to achieve optimal and sustainable use of the subsurface for aquifer thermal energy storage. Energy Policy 2014;66:104–14. https://doi.org/10.1016/j.enpol.2013.11.034.

[15] Ostrom E. A general framework for analyzing sustainability of social-ecological systems. Science 2009;325(5939):419–22. https://doi.org/10.1126/science.1172133.

[16] Jaxa-Rozen M, Kwakkel J, Bloemendal M. The adoption and diffusion of common-pool resource-dependent technologies: the case of aquifer thermal energy storage systems. 2015 Portland international conference on management of engineering and technology (PICMET) 2015. p. 2390–408. https://doi.org/10.1109/PICMET.2015.7273176.

[17] Ma Y, Borrelli F, Hencey B, Coffey B, Bengea S, Haves P. Model predictive control for the operation of building cooling systems. IEEE Trans Control Systems Technol 2012;20(3):796–803.

[18] Farahani SS, Lukszo Z, Keviczky T, De Schutter B, Murray RM. Robust model predictive control for an uncertain smart thermal grid. In: Control conference (ECC), 2016 European; 2016. p. 1195–200.

[19] Rostampour V, Keviczky T. Probabilistic energy management for building climate comfort in smart thermal grids with seasonal storage systems. IEEE Transactions on Smart Grid. arXiv preprint arXiv:1611.03206.

[20] Doughty C, Hellström G, Tsang CF, Claesson J. A dimensionless parameter approach to the thermal behavior of an aquifer thermal energy storage system. Water Resour Res 1982;18(3):571–87.

[21] Ceric A, Haitjema H. On using simple time-of-travel capture zone delineation methods. Groundwater 2005;43(3):408–12. https://doi.org/10.1111/j.1745-6584.2005.0035.x.

[22] Sommer W, Valstar J, van Gaans P, Grotenhuis T, Rijnaarts H. The impact of aquifer heterogeneity on the performance of aquifer thermal energy storage. Water Resour Res 2013;49(12):8128–38. https://doi.org/10.1002/2013WR013677.

[23] Rostampour V, Keviczky T. Distributed stochastic model predictive control synthesis for large-scale uncertain linear systems. 2018 Annual American Control Conference (ACC). IEEE; 2018. p. 2071–7.

[24] Wilensky U. NetLogo; 1999.

[25] Harbaugh AW. MODFLOW-2005, the US Geological Survey modular ground-water model: the ground-water flow process, U.S. Geological Survey; 2005.

[26] Langevin CD, Thorne Jr DT, Dausman AM, Sukop MC, Guo W. SEAWAT Version 4: a computer program for simulation of multi-species solute and heat transport. Tech. rep., U.S. Geological Survey; 2008.

[27] Bakker M, Post V, Langevin CD, Hughes JD, White JT, Starn JJ, et al. Scripting MODFLOW model development using python and FloPy. Groundwater 2016. https://doi.org/10.1111/gwat.12413. n/a–n/a.

[28] Lofberg J. YALMIP: a toolbox for modeling and optimization in MATLAB. Computer aided control systems design, 2004 IEEE international symposium on. 2004. p. 284–9.

[29] van Vliet E. Flexibility in heat demand at the TU Delft campus smart thermal grid with phase change materials Master's thesis Delft University of Technology; 2013.

[30] Ananduta WW. Distributed energy management in smart thermal grids with uncertain demands Master's thesis Delft University of Technology; 2016.

[31] Rostampour V, Bloemendal JM, Keviczky T. A model predictive framework of Ground Source Heat Pump coupled with Aquifer Thermal Energy Storage System in heating and cooling equipment of a building. In: 12th IEA heat pump conference.

[32] Borren W. Ontwikkeling HDSR hydrologisch modelinstrumentarium - HYDROMEDAH. Deelrapport 1: Beschrijving MODFLOW model, Tech. rep., Deltares, Utrecht; 2009.

[33] Gunnink JL. Deklaagmodel en geohydrologische parametrisatie voor het beheersgebied van het Hoogheemraadschap De Stichtse Rijnlanden, Tech. rep., TNO, Utrecht; 2004.

[34] Bloemendal M, Jaxa-Rozen M, Rostampour V. Improved performance of heat pumps helps to use full potential of subsurface space for Aquifer Thermal Energy Storage. In: 12th IEA Heat Pump Conference; 2017.

[35] Bloemendal M, Hartog N. Analysis of the impact of storage conditions on the thermal recovery efficiency of low-temperature ATES systems. Geothermics 2018;71:306–19. https://doi.org/10.1016/j.geothermics.2017.10.009.

[36] Eurostat, Electricity prices for non-household consumers - bi-annual data, Tech. Rep. Dataset NRG_PC_205; 2018.

[37] Eurostat, Gas prices for non-household consumers - bi-annual data, Tech. Rep. Dataset NRG_PC_203; 2018.

[38] Véliz C, Grunewald P. Protecting data privacy is key to a smart energy future. Nature Energy 2018:1. https://doi.org/10.1038/s41560-018-0203-3.

[39] Samad T, Kiliccote S. Smart grid technologies and applications for the industrial sector. Comput Chem Eng 2012;47:76–84. https://doi.org/10.1016/j.compchemeng.2012.07.006.

[40] Rostampour V, Ferrari R, Teixeira A, Keviczky T. Privatized distributed anomaly detection for large-scale nonlinear uncertain systems. IEEE Trans Automatic Control (submitted for publication), 2018.